A Comprehensive Criterion for Threshold of Motion of Bioclastic Sediments under Steady Unidirectional Flow

Lilei Mao[1], Jiabo Li[1], and Yoshimitsu Tajima[1]

[1]The University of Tokyo

December 26, 2023

Abstract

The threshold of motion of bioclastic sediments is the fundamental aspect for understanding of sediment dynamics in coral reef systems while there are currently few studies on its prediction. We conducted laboratory experiments, and showed that the threshold of motion of coral skeletal grains is more appropriately characterized by the nominal diameter and particle density that is defined as the density of grains with its skeletal void filled by the fluid. Distinctions in threshold of motion of observed coral particles and other bioclastic sediments arise from the influences of grain density and shape, resulting in a notable departure from existing empirical thresholds based on quartz sand. We then propose a new formula for estimating critical shear velocity of bioclastic sediments by introducing a grain shape parameter. The new comprehensive criterion improves the understanding of threshold of motion of bioclastic sediments with highly heterogeneous properties under steady unidirectional flow.

Hosted file

982710_0_art_file_11707717_s61vnq.docx available at https://authorea.com/users/711276/articles/695797-a-comprehensive-criterion-for-threshold-of-motion-of-bioclastic-sediments-under-steady-unidirectional-flow

A Comprehensive Criterion for Threshold of Motion of Bioclastic Sediments under Steady Unidirectional Flow

Lilei Mao, Jiabo Li, and Yoshimitsu Tajima

Department of Civil Engineering, The University of Tokyo, 7-3-1 Hongo, Bunkyo City, Tokyo, 113-8654, Japan.

Corresponding author: Yoshimitsu Tajima (yoshitaji@coastal.t.u-tokyo.ac.jp)

Key Points:

- We recommend determining threshold criteria for skeletal coral grains as functions of particle density and nominal diameter.
- Distinctions in threshold of motion of bioclastic sediments and quartz sand primarily arise from the influences of grain density and shape.
- A new comprehensive criterion improves the prediction of threshold of bioclastic grain motion under steady unidirectional flow.

Abstract

The threshold of motion of bioclastic sediments is the fundamental aspect for understanding of sediment dynamics in coral reef systems while there are currently few studies on its prediction. We conducted laboratory experiments, and showed that the threshold of motion of coral skeletal grains is more appropriately characterized by the nominal diameter and particle density that is defined as the density of grains with its skeletal void filled by the fluid. Distinctions in threshold of motion of observed coral particles and other bioclastic sediments arise from the influences of grain density and shape, resulting in a notable departure from existing empirical thresholds based on quartz sand. We then propose a new formula for estimating critical shear velocity of bioclastic sediments by introducing a grain shape parameter. The new comprehensive criterion improves the understanding of threshold of motion of bioclastic sediments with highly heterogeneous properties under steady unidirectional flow.

Plain Language Summary

The shorelines of coral reef islands are composed of various biotype sediments, which are derived from shells and marine organisms such as corals. These sediment grains have different size, density and shape characteristics compared with quartz sand. Understanding the threshold condition at which these sediments initiate to move is essential for prediction of transport and topography changes of coral beach. We used a series of data of preceding studies and our newly conducted experiments to investigate appropriate grain proprieties that well characterize the threshold of motion of coral skeletal grains, and found that particle density and nominal diameter are better than solid density and sieve diameter for determination of the threshold. Finally, we proposed a new comprehensive criterion of the threshold of motion of arbitrary particles including bioclastic grains, accounting for the grain shape effect and the settling velocity difference.

1 Introduction

Coral reef islands, also known as coral cays or atolls, have unique landforms of wave-transported coral debris, sand, and organic material on the surface of submerged coral reefs (Masselink et al., 2020), which are typically found in tropical and subtropical regions. Marine carbonate grains that contribute to the composition of coral coasts are primarily derived from the shells and skeletons of marine organisms like corals, mollusks, and foraminifera (East et al., 2018; Masselink et al., 2021), and are accumulated along nearshore areas through complex hydrodynamic processes driven by nearshore currents and wave actions (Bonesso et al., 2022). Climate change and human activities pose a severe threat to the biodiversity of coral reefs, significantly disrupting the process of carbonate grain accumulation and exerting detrimental effects on coastal stability (Quataert et al., 2015; Ferrigno et al., 2016). These bioclastic sediments exhibit heterogenous density, break-down size, and shape characteristics (Chazottes et al., 2008), and understanding the transport characteristics of these sediments is vital for prediction of beach deformation of coral coast.

The prediction of threshold of sediment motion is a fundamental aspect in the study of sediment transport mechanisms. Since the pioneering work of Shields (1936), numerous experiments have been performed to investigate the threshold of motion of both natural and artificial particles on flat beds under virous flow conditions, including steady unidirectional flow and wave-associated orbital oscillatory current flow. Shields curve determines the critical Shields parameter, defined as nondimensional critical shear stress, as a function of a grain Reynolds number. Following the original Shields curve, Paphitis (2001) proposed threshold curves and envelopes to account for the irregular shape of natural particles. Compared to quartz sediments, few studies have investigated the threshold of motion of marine carbonate grains despite their widespread presence in modern and past marine sedimentary environments.

Experimental studies on threshold of motion of bioclastic sediments have shown the influence of irregular grain shape on their initiation motion conditions by examining the discrepancy between obtained critical Shields parameter and the existing Shields curve established for quartz sediments (e.g., Rieux et al., 2019; Bian et al., 2023). Some of these preceding studies used alternative grain diameters, e.g., nominal diameter, equivalent settling diameter, to account for the shape effect in formulation of the threshold criteria (e.g., Smith and Cheung, 2004; Weill et al., 2010). Additionally, Movability number, defined as a ratio of shear velocity to settling velocity, was suggested as an alternative parameter for determination of sediment motion threshold (e.g., Beheshti and Ataie-Ashtiani, 2008; Simões, 2014) since it may have a merit in accounting for the influence of settling velocity of sediment grains on their threshold of motion. However, none of them has gained universal recognition as generic threshold criteria of various grains. Further modifications may be required for these preceding criteria to enhance their applicability to bioclastic sediments.

In this study, our objective is to quantify the influence of grain density and shape on the determination of threshold criteria for bioclastic sediments and to propose a new comprehensive criterion for estimating critical shear velocity of bioclastic sediments with highly heterogeneous properties by introducing a grain shape parameter. To achieve this objective, we experimentally investigate the threshold of motion of coral particles and compare the obtained critical conditions with those of preceding studies.

2 Materials and Methods

2.1 Coral debris samples

We obtained natural coral debris samples from an aquarium market, which were originally from Okinawa Prefecture, Japan. The source samples were dried and then sieved into five size fractions (Figure S1), including 5.60 mm to 6.70 mm (PS1), 4.75 mm to 5.60 mm (PS2), 4.00 mm to 4.75 mm (PS3), 3.35 mm to 4.00 mm (PS4), and 2.00 mm to 3.35 mm (PS5). We measured density of original samples using a 50 ml pycnometer and the average solid density ρ_{solid} was measured to be 2.49±0.23 g/cm^3. However, the density of bioclastic grains is notably affected by their skeletal structures. In this study, we use the particle density ρ_{p}, defined in Equation 1, for determination of sediment transport characteristics (Cuttler et al., 2017).

$$\rho_{\mathrm{p}} = \rho_{\mathrm{solid}}(1-\varphi) + \rho\varphi \tag{1}$$

Here, φ is the skeletal porosity, and ρ is the fluid density. The average φ of present coral debris sample was measured to be 0.42, resulting in the average ρ_{p} of 1.87±0.13 g/cm^3 (Mao et al., 2023).

The sieve diameter d_{sv} for each size fraction was determined based on a logarithmic distribution of sizes between the adjacent sieves. The commonly used size descriptor for irregularly shaped particles, the nominal diameter d_n, is defined as the diameter of a sphere whose volume is equivalent to that of a non-spherical particle, calculated by $d_n = (d_l d_i d_s)^{1/3}$, where d_l, d_i and d_s represent the diameters in the longest, intermediate, and shortest mutually perpendicular axes, respectively. We built a three-dimensional image acquisition system to measure d_l, d_i, d_s and maximum projected area A_{mp}, of coral particles, and further determined several particle shape parameters, i.e. particle flatness d_s/d_i, elongation d_i/d_l, Corey shape factor S_f $(= d_s/(d_l d_i)^{1/2})$.

The settling velocity w_s, of coral particles was determined through settling tube experiments. A detailed description of the particle shape measurement and settling tube experimental method can be found in Mao et al. (2023). We measured the particle shape and settling velocity for over 35 particles in each coral debris sample. These particles covered the largest and the smallest grains in each sample. The average values of obtained particle size, shape parameters and settling velocity were used in subsequent calculations for each sample.

2.2 Experimental setup

Threshold experiments were performed in the oscillatory flow tunnel (OFT, Figure 1a) at the Coastal Engineering Laboratory of the University of Tokyo, which consists of a loop-shape closed conduit. The OFT is equipped with a 570 cm-long and 23.3 cm-high horizontal test section with a glass sidewall on the observational side and a black wooden background board. The test section has a 430 cm-long, 7.6 cm-wide, and 10 cm-deep pocket filled by sediment to create the movable bed. At both ends of the movable bed section, ramps were respectively placed which smoothly connects the movable bed and the fixed bed of the tunnel floor. Sediment traps made of honeycombs were placed at the end of both sides of the test section. In this experiment, movable bed with thickness of 10 cm was created by the five sets of coral debris samples, and unidirectional flow was generated by the pump. The flow velocity was gradually increased until the coral particles initiate to move.

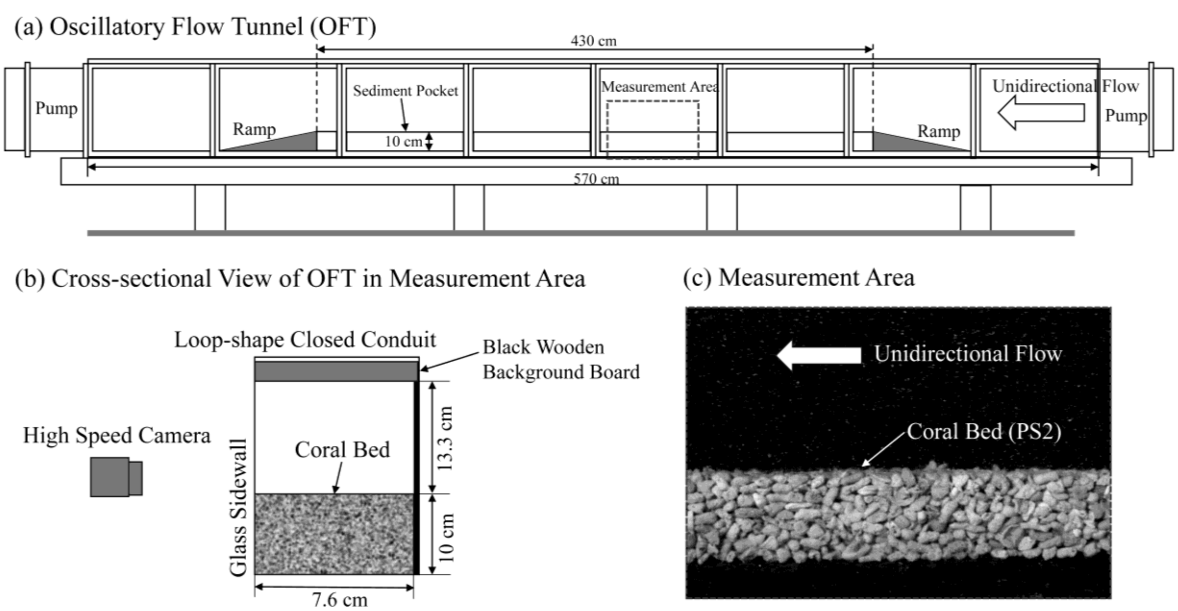

Figure 1. Layout of the threshold experimental setup in the oscillatory flow tunnel.

The flow field over the bed was quantified within a rectangular measurement area near the middle part of the test section using a two-dimensional particle image velocimetry (PIV) system. The water was seeded using non-polar crosslinked polymer with a diameter of 0.35 mm and the density nearly identical to the water. Two spotlights were used to illuminate the observation section. The camera was aligned at the average bed level looking normal to the side glass wall (Figure 1b), so that the obtained image accurately captures the streamwise horizontal and vertical flow velocity components. The camera was operated at a frame rate of 120 fps and captured the flow field images with 640×480 pixels in each frame (Figure 1c), which covers the area of 19.4×14.6 cm on the side glass wall.

We adopted the quantitative criterion ε (Equation S1) proposed by Yalin (1972) to determine the threshold of motion of coral particles based on the aforementioned video images. The number of grains detached from the bed in a time Δt, over a given area A, of the bed can be estimated by Equation S1, which in turn determines the threshold condition in the experiment. In this study, Δt =120 sec, A =0.0266 m^2, and $\varepsilon \geq 10^{-6}$ were applied to determine the threshold of sediment motion, and the characteristic grain diameter d has been taken as d_n of each sample.

A double-averaging method (DAM) (Nikora et al., 2007) was employed to analyze the measured flow field over the coral bed. The bed shear velocity, u_*, can be calculated from the double-averaged (DA) velocity profile within the boundary layer based on the law of the wall (Equation S2). The structure of the boundary layer depends on the hydraulic regime of the flow, which is determined by the shear Reynolds number R_* ($= u_* k_s/\nu$, where k_s is the Nikuradse roughness length and ν is kinetic viscosity of the fluid). The Nikuradse roughness length for hydraulically rough flows is then determined by $k_s = 30z_0$ (Van Rijn, 1993), where z_0 is the level where the DA streamwise horizontal velocity is zero.

To compare the threshold of motion of coral particles to other sediment grains, the threshold criteria are represented by critical Shields parameter θ_{cr} and critical Movability number Λ_{c}, which are respectively defined by,

$$\theta_{\mathrm{cr}} = \frac{\rho u_{*\mathrm{cr}}^2}{(\rho_s - \rho) g d} \tag{2}$$

$$\Lambda_{\mathrm{c}} = \frac{u_{*\mathrm{cr}}}{w_s} \tag{3}$$

where ρ_s is the sediment density, and $u_{*\mathrm{cr}}$ is the critical shear velocity. Obtained θ_{cr} can be plotted as a function of either the grain Reynolds number Re_* ($= u_* d/\nu$) or the dimensionless grain diameter d_* ($= [(\rho_s - \rho) g/\rho\nu^2]^{1/3} d$) (Paphitis, 2001). Experimental parameters at the threshold of motion of the five coral debris samples are reported in Table S1.

3 Results and Discussion

3.1 Characterization of particle size, shape, and bed roughness length

Figures 2 show characteristics of various grain sizes and shapes of five sets of coral debris samples sorted through sieving. As seen in Figure 2a and Table S1, despite different size ranges, average values of S_f of coral particles in the five samples were close to each other within 0.26≤ S_f ≤0.72, and these S_f values significantly differ from that of the spherical particle ($S_f = 1$). In Figure 2b, the mean intermediate diameter d_i and sieve diameter d_{sv} were linearly correlated, and d_i of all five samples were larger than d_{sv}. Similarly, good linear correlation was found between d_n and d_i (Figure 2c) and between d_n and d_{sv} (Figure 2d) regardless of their particle shapes. The values of d_n were larger than corresponding d_{sv}. These results indicate that the flatness (d_s/d_i) of these sample grains were larger than their elongation (d_i/d_l). This feature also supports the predominance of rod-shaped particles in the five coral debris samples seen in Figure 2a. The obtained linear correlations enable us to reasonably estimate d_i and d_n of coral debris samples as a function of commonly used d_{sv}.

Figure 2e shows a clear correlation between S_f and the particle flatness d_s/d_i. Compared to spherical particles, flatter particles have relatively lower effective roughness height, and thus induce lower shear velocities under the same depth-averaged flow velocity. Additionally, we estimated A_{mp} of sample coral particles, which relates to the drag force acting on these particles. Figure 2f shows the plot of observed A_{mp} of coral particles as a function of their d_n. It is evident that A_{mp} of coral particles are larger than that of spherical particle with its diameter represented by d_n, shown in a solid line curve.

Relatively large shear Reynolds number, $R_* > 70$, reported in Table S1, indicates that the flow over the coral bed in the experiment is rough-turbulent flow. We obtained the Nikuradse roughness length, k_s, for the five coral beds, and investigated the correlation between estimated k_s and the characteristic grain diameter, d_{sv} or d_n of the coral bed (Figure S2). Good linear correlations were found between k_s and either d_{sv} or d_n for coral beds. It can be reasonably expected that k_s can be determined by any of aforementioned particle diameters since these diameters are also linearly correlated with each other (Figures 2b~2d). The obtained correlations were $k_s \approx 2.68 d_n$ (R^2 =0.99) and $k_s \approx 3.51 d_{sv}$ (R^2 =0.99). The proportionality factor between k_s and d_n was reasonably consistent with Nielsen's (1992) formula ($k_s = 2.5 d_{50}$, where d_{50} is the particle median diameter) for quartz round sand grains. Considering the influence of particle shape difference, we recommend d_n to represent the characteristic size of irregularly shaped coral particles for estimation of k_s and so as threshold criteria. However, further investigation may be required for general merit of d_n since most of existing studies are based on d_{sv} (Weill et al., 2010; Rieux et al., 2019) and the number of studies using d_n is limited.

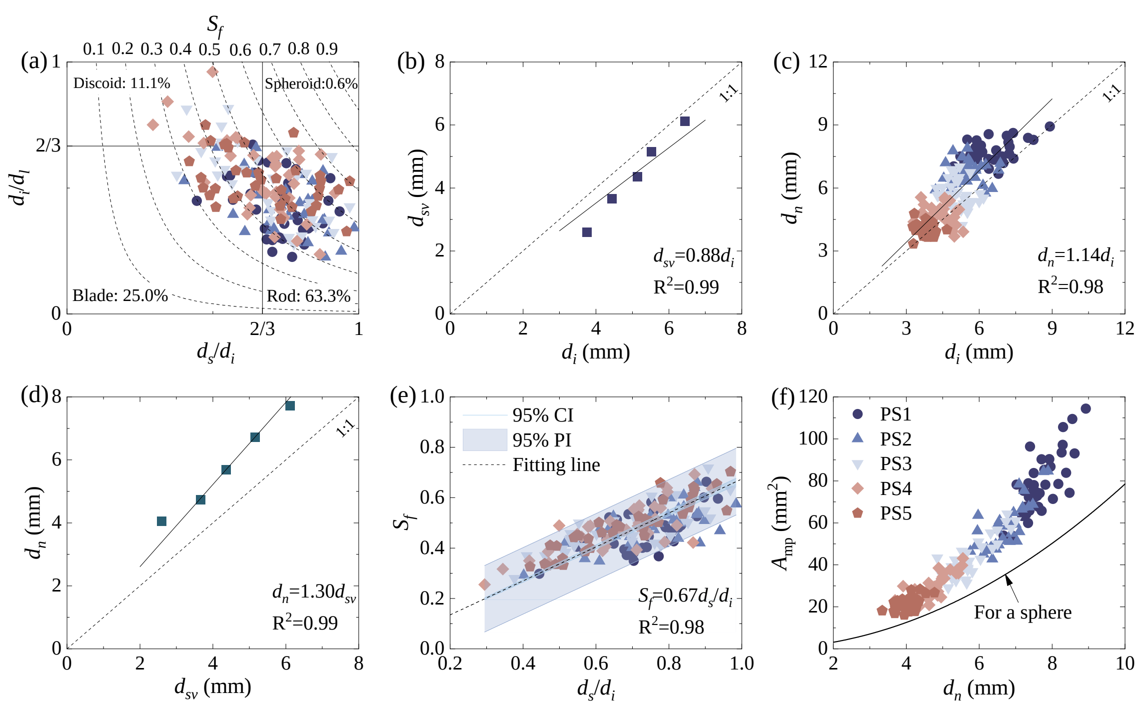

Figure 2. Particle size and shape characterization of coral debris samples used in the experiments. (a) Particle shape distribution for each coral debris sample plotted in Zingg classification diagram (1935), where contour lines of the Corey shape factor are shown with their values specified along the top axis. (b) Sieve diameter versus intermediate diameter. (c) Nominal diameter versus intermediate diameter. (d) Nominal diameter versus sieve diameter. (e) Correlation between the Corey shape factor and particle flatness. (f) Relationship between the maximum projected areas A_{mp}, of the particles in the five coral debris samples and their nominal diameters.

3.2 Appropriate grain properties for determination of threshold of bioclastic grain motion

We first calculated critical Shields parameter θ_{cr}, for coral particles using Equation 2 with measured $u_{*\mathrm{cr}}$, $\rho_{\mathrm{s}} = \rho_{\mathrm{p}}$, and $d = d_{sv}$. Figure 3a shows the plot of θ_{cr} for coral particles as a function of d_*. For comparison, this figure shows the plots of θ_{cr} when φ in Equation 1 was set either $\varphi = 0$ and $\varphi = 0.42$. Note that ρ_{p} becomes identical to ρ_{solid} if $\varphi = 0$ is applied. The figure also shows the plots of threshold data of other bioclastic sediments (Table S2 for detailed information) under unidirectional flows (Prager et al., 1996; Paphitis et al., 2002; Smith and Cheung, 2004; Weill et al., 2010; Rieux et al., 2019; Bian et al., 2023). Here $\varphi = 0$ was assumed for these bioclastic grains for determination of ρ_{p} in Figure 3a. While the obtained θ_{cr} based on d_{sv} and ρ_{p} with $\varphi = 0$ for coral particles are close to the empirical curves (Shields, 1936; Paphitis, 2001), the majority of datapoints from preceding studies fall below the empirical curve or even below the lower envelop of Paphitis (2001). For coral particles, values of θ_{cr} increase when the value of φ is changed from 0 to 0.42, and these plots are located even above the upper envelope of Paphitis (2001).

Figure 3b shows the similar plot of θ_{cr} versus d_* for the same particles in Figure 3a but the diameter d in Equation 2 was represented by d_n. An obtained linear relationship $d_n = 1.34 d_{sv}$ (R^2=0.99, Figure S3) was used to estimate d_n of carbonate sand reported by Prager et al. (1996). The d_n values of mollusc fragments (Paphitis et al., 2002; Weill et al., 2010; Rieux et al., 2019) were estimated using $d_n = 0.62 d_{sv}$ (R^2=0.99, Figure S3) based on the shelly particle data of Silva et al. (2023). As seen in the figure, θ_{cr} of coral particles are plotted below the empirical curves (Shields, 1936; Paphitis, 2001) when $\varphi = 0$ is applied. Similarly, datapoints of coral sediment (ρ_{p} =2.82 g/cm^3, $\varphi = 0$) reported by Bian et al. (2023) are also plotted further below the empirical curves (Shields, 1936; Paphitis, 2001) particularly for relatively small d_*. This feature supports our deduction that the grain density neglecting the influence of skeletal porosity, i.e., $\varphi = 0$, is too large to represent the behavior of coral skeletal grains in the fluid. On the other hand, the plot of θ_{cr} versus d_* for coral particles based on ρ_{p} with $\varphi = 0.42$ are slightly above the empirical curves but yet within the 91.1% envelope of Paphitis (2001).

Overall, the use of d_n and ρ_{p} yields θ_{cr} values closer to the empirical curve of Paphitis (2001) (Figure 3b) compared to the use of d_{sv}. From these comparisons, it can be inferred that the combination of d_n and ρ_{p} with appropriate φ would provide a reasonable representation of θ_{cr} for irregular shape coral particles within the range of 4.05 mm$< d_n <$7.72 mm. While one of drawbacks of d_n and ρ_{p} may be in that it is not easy to obtain their accurate values, accurate estimation of φ may yield θ_{cr} more consistent with the empirical curve. On the other hand, the discrepancy of some datapoints (Figure 3b) may also indicate that empirical Shields curves based on θ_{cr} versus d_* (Shields, 1936; Paphitis, 2001) might not be the best parameter to account for the influence of diverse irregularity of various bioclastic sediments.

The Movability number may have merit in determination of the threshold of bioclastic grain motion because of its explicit inclusion of particle settling velocity. Figures 3c and 3d show the plot of the critical Movability number Λ_{c} (Equation 3) as a function of d_* based on d_{sv} (3c) and on d_n (3d), respectively, for the present coral particles, other particles and the empirical curve of Simões (2014). In estimation of Λ_{c}, measured settling velocities were applied except the data reported by Prager et al. (1996), Smith and Cheung (2004) and Bian et al. (2023), in which measured settling velocities were not presented. For these particles, we used the simple formula with their d_n, established for calcareous sand (Equation S3, Alcerreca et al., 2013). The magnitudes of estimated w_s of considered bioclastic grains were smaller than those obtained from the empirical curve based on smooth spheres (Dietrich, 1982).

In Figure 3c, it is evident that the majority of plotted Λ_{c} are higher than the empirical curve. Many of the plotted Λ_{c} of mollusc fragments (Rieux et al., 2019) are higher than the empirical curve by a factor of 2 to 3 whereas some of the plotted θ_{cr} of the same mollusc fragments (Rieux et al., 2019) are more than 10 times lower than the Shields curve (Figure 3a). This opposite difference is because the settling velocity of mollusc fragments is much smaller than that of quartz sand grains.

In Figure 3d, some plots are lower than the empirical curve particularly for relatively small d_* based on d_n. Overall better agreement with empirical curve in Λ_{c} rather than in θ_{cr} indicates the superiority of Λ_{c} which can account for the influence of various different factors of grains through their settling velocity. Thus, the critical Movability number based on ρ_{p} and d_n may have the higher potential as a comprehensive criterion for the threshold of motion of bioclastic sediments.

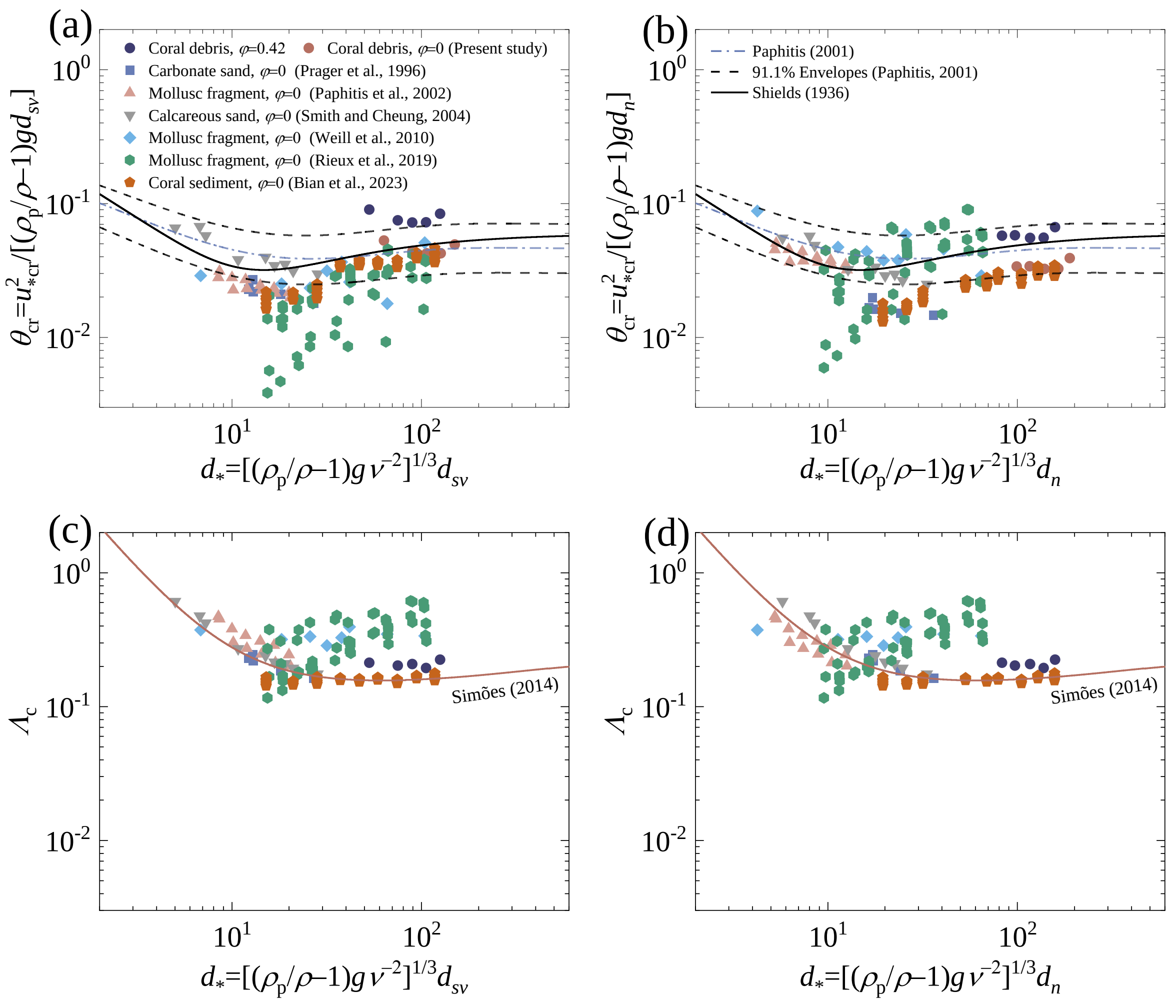

Figure 3. Two threshold criteria, critical Shields parameter θ_{cr} and critical Movability number Λ_{c}, for coral particles (present study), carbonate sand (Prager et al., 1996), mollusc fragments (Paphitis et al., 2002; Weill et al., 2010; Rieux et al., 2019), calcareous sand (Smith and Cheung, 2004), and coral sediment (Bian et al., 2023). (a) Shields plot (θ_{cr} versus d_*) based on ρ_{p} and d_{sv}. (b) Shields plot (θ_{cr} versus d_*) based on ρ_{p} and d_n. (c) Λ_{c} plot as a function of d_* based on d_{sv}. (d) Λ_{c} plot as a function of d_* based on d_n. The plotted empirical threshold curves from Shields (1936), Paphitis (2001) and Simões (2014) were developed for the threshold of motion of quartz grains (ρ_s =2.65 g/cm^3) under unidirectional flows.

3.3 A new comprehensive criterion for threshold of bioclastic grain motion

The determination of Λ_{c} requires the estimation of w_{s} of the particle, which depends on the particle density, shape, angularity, and surface roughness (Dietrich, 1982). Similarly, the value of Λ_{c} may also be affected by these particle characteristics. Accounting for diverse characteristics of particles, we propose a new comprehensive criterion for threshold of motion of bioclastic sediments by,

$$u_{*\mathrm{cr}} = w_s \Lambda_{\mathrm{c}} = w_s \Lambda_{\mathrm{c}0} f(\mathrm{shape}) \tag{4}$$

where w_s is the settling velocity of the target particle, which accounts for the influence of aforementioned various characteristics of each particle, and $\Lambda_{\mathrm{c}0}$ is the existing empirical formula of the critical Movability number (Simões, 2014) determined by,

$$\Lambda_{c0} = 0.215 + \frac{6.79}{d_*^{1.70}} - 0.075e^{-2.62\times10^{-3}d_*} \quad (5)$$

It should be noted that the empirical curve of Simões (2014) is relatively less sensitive to d_* where $d_* > 10$ (Figure 3c), indicating that the choice of d_{sv} or d_n in estimation of Λ_{c0} would yield insignificant difference for relatively large grains of $d_* > 10$. This feature also indicates that the empirical formula (Equation 5) needs further modification to reduce the data dispersion (Figures 3c or 3d) of bioclastic sediments, which may be due to their shape difference. In Equation 4, therefore, $f(\text{shape})$ accounts for the influence of different particle shape on Λ_c while $f(\text{shape}) = 1$ for spherical particles.

Taking the logarithm of Equation 4, the following general form is given,

$$\log u_{*cr} = \log \Lambda_{c0} + \log w_s + a\log F \quad (6)$$

where a is the fitting coefficient, and F represents a parameter such as S_f, accounting for the shape difference. Following Mao et al. (2023), a ratio of dimensionless settling velocity of an arbitrary particle w_* $(= [(\rho_s - \rho)g\nu/\rho]^{-1/3}w_s)$ to that of a volume-equivalent sphere particle w_{*0}, can also be a candidate option of F, i.e., $F = w_*/w_{*0}$. Estimated w_*/w_{*0} of bioclastic grains in this study are smaller than unity (Figure S4), and thus the shelly particles (Paphitis et al., 2002; Weill et al., 2010; Rieux et al., 2019) are expected to have rather smaller w_*/w_{*0}, suggesting a more pronounced influence of $F = w_*/w_{*0}$ on threshold of sediment motion.

To achieve the best prediction of u_{*cr}, we conducted regression analysis of Equation 6 under different scenarios (Table S3). We assessed the influence of grain shape on prediction of u_{*cr} for present coral grain dataset. When representing F by S_f or, w_*/w_{*0}, Equation 6 yields more accurate prediction of u_{*cr} compared to the scenario with $F = 1$, i.e., $\Lambda_c = \Lambda_{c0}$. Based on the datasets of present coral particles, carbonate sand (Prager et al., 1996), calcareous sand (Smith and Cheung, 2004), and mollusc fragments (Paphitis et al., 2002; Weill et al., 2010; Rieux et al., 2019), we found that $F = w_*/w_{*0}$ yields the best fit formula (R^2 =0.972) given by,

$$u_{*cr} = \Lambda_{c0} w_s \left(\frac{w_*}{w_{*0}}\right)^{-0.589} \quad (7)$$

Figure 4 shows the comparisons of observed u_{*cr} with predicted u_{*cr} when $F = 1$, i.e., $\Lambda_c = \Lambda_{c0}$ and the proposed formula (Equation 7). Our proposed formula (Equation 7) yields a lower absolute relative error (ARE) of 14.81%, than the one based on Λ_{c0} with ARE of 35.64%. Either d_{sv} or d_n can be applied for estimation of d_* in Equation (5). As was discussed in the previous section, the choice of either d_{sv} or d_n showed insignificant difference and equally low ARE were obtained in both cases. Considering the limited available information on grain properties, more precise data about skeletal porosity, nominal diameter and shape parameters would further enhance the precision of predicting critical shear velocity using Equation 7 for bioclastic sediments with different size, density and shape.

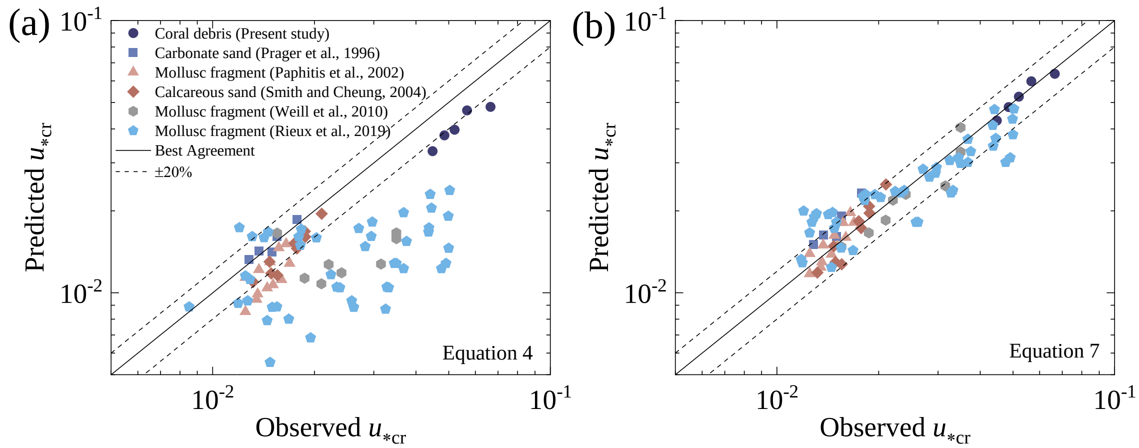

Figure 4. (a) Comparison of observed $u_{*\mathrm{cr}}$ with predicted $u_{*\mathrm{cr}}$ when $F = 1$ in Equation 4. (b) Comparison of observed $u_{*\mathrm{cr}}$ with predicted $u_{*\mathrm{cr}}$ using proposed formula (Equation 7).

4 Conclusions

Our experimental findings from natural coral debris sample, along with compiled data of other bioclastic sediments suggest that the use of particle density and nominal diameter could improve the determination of critical Shields parameter. We quantified the effects of grain density and shape on deriving the threshold criteria for bioclastic sediments versus quartz sand. A new formula for estimating the critical shear velocity of bioclastic sediments was proposed by introducing a grain shape parameter based on the concept of critical Movability number. The new comprehensive criterion improves the predictive skills of threshold of motion of bioclastic sediments under steady unidirectional flow, which may enhance the accurate modeling of sediment dynamics in coral reef systems.

Acknowledgments

This work was supported by JSPS under the Joint Research Program implemented in association with NSFC (JRP with NSFC). Grant Number: JPJSJRP 20191802.

Data Availability Statement

Data presented in this paper are available at Zenodo via https://doi.org/10.5281/zenodo.10398426.

References

Alcerreca, J.C., Silva, R., & Mendoza, E. (2013). Simple settling velocity formula for calcareous sand. *Journal of Hydraulic Research*, 51(2), 215-219. doi: 10.1080/00221686.2012.753645

Beheshti, A.A., & Ataie-Ashtiani, B. (2008). Analysis of threshold and incipient conditions for sediment movement. *Coastal Engineering*, 55(5), pp.423-430. doi: 10.1016/j.coastaleng.2008.01.003

Bian, C., Chen, J., Jiang, C., Wu, Z., & Yao, Z. (2023). Threshold of motion of coral sediment under currents in flume experiments. *Sedimentology*. doi: 10.1111/sed.13082

Bonesso, J.L., Browne, N.K., Murley, M., Dee, S., Cuttler, M.V., Paumard, V., Benson, D., & O'Leary, M. (2022). Reef to island sediment connections within an inshore turbid reef island system of the eastern Indian Ocean. *Sedimentary Geology*, 436, p.106177. doi: 10.1016/j.sedgeo.2022.106177

Chazottes, V., Reijmer, J.J.G., & Cordier, E. (2008). Sediment characteristics in reef areas influenced by eutrophication-related alterations of benthic communities and bioerosion processes. *Marine Geology*, 250 (1-2), 114-127. doi: 10.1016/j.margeo.2008.01.002

Cuttler, M.V., Lowe, R.J., Falter, J.L., & Buscombe, D. (2017). Estimating the settling velocity of bioclastic sediment using common grain-size analysis techniques. *Sedimentology*, 64(4), 987-1004. doi:10.1111/sed.12338

Dietrich, W.E. (1982). Settling velocity of natural particles. *Water Resources Research*, *18*(6), 1615-1626. doi: 10.1029/WR018i006p01615

East, H.K., Perry, C.T., Kench, P.S., Liang, Y., & Gulliver, P. (2018). Coral reef island initiation and development under higher than present sea levels. *Geophysical Research Letters*, 45(20), pp.11-265. doi: 10.1029/2018GL079589

Ferrigno, F., Bianchi, C.N., Lasagna, R., Morri, C., Russo, G.F., & Sandulli, R. (2016). Corals in high diversity reefs resist human impact. *Ecological Indicators*, 70, pp.106-113. doi: 10.1016/j.ecolind.2016.05.050

Mao, L.L., Li, J.B., Shimozono, T., & Tajima, Y. (2023). Impacts of Particle Shape, Skeletal Porosity and Density on the Settling Velocity of Gravel-Size Coral Debris. *Journal of Geophysical Research: Earth Surface*, 128(5), e2022JF006996. doi: 10.1029/2022JF006996

Masselink, G., Beetham, E., & Kench, P. (2020). Coral reef islands can accrete vertically in response to sea level rise. *Science Advances*, 6(24), p.eaay3656. doi: 10.1126/sciadv.aay3656

Masselink, G., McCall, R., Beetham, E., Kench, P., & Storlazzi, C. (2021). Role of future reef growth on morphological response of coral reef islands to sea-level rise. *Journal of Geophysical Research: Earth Surface*, 126(2), p.e2020JF005749. doi: 10.1029/2020JF005749

Nielsen, P. (1992). Coastal Bottom Boundary Layers and Sediment Transport, Advanced Series on Ocean Engineering-Vol. 4. World Scientific: Singapore; 324 pp.

Nikora, V., McEwan, I., McLean, S., Coleman, S., Pokrajac, D., & Walters, R. (2007). Double-averaging concept for rough-bed open-channel and overland flows: Theoretical background. *Journal of Hydraulic Engineering*, 133(8), pp.873-883. doi: 10.1061/(ASCE)0733-9429(2007)133:8(873)

Paphitis, D. (2001). Sediment movement under unidirectional flows: an assessment of empirical threshold curves. *Coastal Engineering*, 43(3-4), pp.227-245. doi: 10.1016/S0378-3839(01)00015-1

Paphitis, D., Collins, M.B., Nash, L.A., & Wallbridge, S. (2002). Settling velocities and entrainment thresholds of biogenic sands (shell fragments) under unidirectional flow. *Sedimentology*, 49(1), pp.211-225. doi: 10.1046/j.1365-3091.2002.00446.x

Prager, E.J., Southard, J.B., & VivoniGallart, E.R. (1996). Experiments on the entrainment threshold of well-sorted and poorly sorted carbonate sands. *Sedimentology*, 43(1), pp.33-40. doi: 10.1111/j.1365-3091.1996.tb01457.x

Quataert, E., Storlazzi, C., Van Rooijen, A., Cheriton, O., & Van Dongeren, A. (2015). The influence of coral reefs and climate change on wave-driven flooding of tropical coastlines. *Geophysical Research Letters*, 42(15), pp.6407-6415. doi: 10.1002/2015GL064861

Rieux, A., Weill, P., Mouaze, D., Poirier, C., Nechenache, F., Perez, L., & Tessier, B. (2019). Threshold of motion and settling velocities of mollusc shell debris: Influence of faunal composition. *Sedimentology*, 66(3), pp.895-916. doi:10.1111/sed.12521

Shields, A. (1936). Application of Similarity Principles and Turbulence Research to Bed-load Movement (English Translation of the original German Manuscript). Hydrodynamics Laboratory, California Institute of Technology, Publication No. 167.

Silva, F.R.S.D., Borges, A.L.D.O., Toldo Jr, E.E., Fick, C., Puhl, E., Oliveira, V.C.B., & Cruz, F.E.G.D. (2023). Threshold of motion and orientation of bivalve shells under current flow. *Brazilian Journal of Geology*, 53, p.e20220080. doi: 10.1590/2317-4889202320220080

Simões, F.J. (2014). Shear velocity criterion for incipient motion of sediment. *Water Science and Engineering*, 7(2), pp.183-193. doi: 10.3882/j.issn.1674-2370.2014.02.006

Smith, D.A., & Cheung, K.F. (2004). Initiation of motion of calcareous sand. *Journal of Hydraulic Engineering*, 130(5), pp.467-472. doi: 10.1061/(ASCE)0733-9429(2004)130:5(467)

Van Rijn, L. (1993). Principles of Sediment Transport in Rivers, Estuaries and Coastal Seas. Aqua Publications, Amsterdam, The Netherlands, 690 pp.

Weill, P., Mouazé, D., Tessier, B., & Brun-Cottan, J.C. (2010). Hydrodynamic behaviour of coarse bioclastic sand from shelly cheniers. *Earth Surface Processes and Landforms*, 35(14), pp.1642-1654. doi: 10.1002/esp.2004

Yalin, M.S. (1972). Mechanics of Sediment Transport. Pergamon Press, New York, 290 pp.

Zingg, T. (1935). Beitrag zur Schotteranalyse. *Doctoral dissertation, ETH Zurich*. doi: 10.3929/ethz-a-000103455

References From the Supporting Information

Padhi, E., Penna, N., Dey, S., & Gaudio, R. (2018). Hydrodynamics of water-worked and screeded gravel beds: A comparative study. *Physics of Fluids*, 30(8). doi: 10.1063/1.5044479

Geophysical Research Letters

Supporting Information for

A Comprehensive Criterion for Threshold of Motion of Bioclastic Sediments under Steady Unidirectional Flow

Lilei Mao, Jiabo Li, and Yoshimitsu Tajima

Department of Civil Engineering, The University of Tokyo, 7-3-1 Hongo, Bunkyo City, Tokyo, 113-8654, Japan.

Corresponding author: Yoshimitsu Tajima (yoshitaji@coastal.t.u-tokyo.ac.jp)

Contents of this file

Text S1 to S4
Figures S1 to S5
Tables S1 to S3

Text S1

The threshold of sediment motion is determined as the critical condition under which a bed surface materials initiate to move under the unidirectional flow. However, there is no universally accepted criteria for defining the initiation of the sediment motion, leading to discrepancies in previous datasets. In this study, we adopted the quantitative criteria ε proposed by Yalin (1972) to determine the threshold of motion of coral particles based on the video images recorded in the experiment. The dimensionless parameter ε is defined as,

$$\varepsilon = \left(\frac{N}{A\Delta t}\right)\left[\frac{\rho d^5}{(\rho_\mathrm{p} - \rho)g}\right]^{1/2} \tag{S1}$$

where N is the number of grains detached from the bed in the time Δt, over the given bed surface area, A, g is the gravitational acceleration, and d is the characteristic grain diameter of the sediment. The value of ε was suggested to be small, on the order of 10^{-6}. Then, the value of N for each sample can be estimated, which in turn determines the threshold condition of the initiation of sediment motion in the experiments. In this study, Δt =120 sec, A =0.0266 m^2, and $\varepsilon \geq 10^{-6}$ was applied to determine the sediment threshold of motion, and d has been taken as the nominal diameter d_n of each sample.

Text S2

In the context of flows over rough beds, conventional Reynolds equations or Reynolds averaged Navier-Stokes equations are inadequate due to the spatial heterogeneity observed in the near-bed region (Padhi et al., 2018). To address this complexity, the time averaging is conceptually supplemented by the area averaging in the layer parallel to the mean bed surface, which is called a double-averaging method (DAM) (Nikora et al., 2007). With DAM, the local instantaneous horizontal and vertical velocities (u, w) are separated into a time-averaged velocity quantity ($\bar{u}$, $\bar{w}$) and a turbulent fluctuation (u', w') by Reynolds decomposition. Then, the horizontally varying time-averaged velocities ($\bar{u}$, $\bar{w}$) are decomposed as a double-averaged (DA) velocity ($\langle\bar{u}\rangle$, $\langle\bar{w}\rangle$), averaged over horizontal space, and a horizontal fluctuation of the time-averaged velocity ($\tilde{u}$, $\tilde{w}$). In this study, the DAM was employed to analyze the flow field over the coral debris bed.

The near-bed turbulent boundary layer governs the particle motion at the bed. The bed shear velocity, u_*, can be calculated from the double-averaged (DA) velocity profile within the boundary layer based on the law of the wall. The structure of the boundary layer depends on the hydraulic regime of the flow, which is determined by the shear Reynolds number R_*=$u_* k_s/\nu$, where k_s is the Nikuradse roughness length and ν is kinetic viscosity of the fluid. The law of the wall is defined as follows,

$$\frac{\langle\bar{u}\rangle}{u_*} = \frac{1}{\kappa}\ln\left(\frac{z}{z_0}\right) \tag{S2}$$

where $\langle\bar{u}\rangle$ is the DA streamwise horizontal velocity, κ is the von Kármán constant (=0.41), z is the elevation from the origin $z = 0$ determined at the gravel crest on the bed surface, and z_0 is the level where $\langle\bar{u}\rangle = 0$. With the measured $\langle\bar{u}\rangle$ and corresponding z within the logarithmic layer, the values of u_* and z_0 are obtained by the linear regression line of $\langle\bar{u}\rangle$ and $\ln(z)$ using Equation S2.

Text S3

Alcerreca et al. (2013) proposed a simple equation for the computation of particle settling velocity based on the dataset of 1557 calcareous sand grains, which is expressed as,

$$\frac{w_s d}{\nu} = \left(\sqrt{22 + 1.13d_*^2} - 4.67\right)^{1.5} \tag{S3}$$

where $d_* = [(\rho_s - \rho)g/\rho\nu^2]^{1/3}d$, and d is taken as d_n in his study.

Text S4

Dietrich (1982) presented the fourth-order polynomial fitted equation of the relationship between d_* and w_{*0} for spherical particles, expressed as

$$\begin{aligned}\log W_{*0} = &-3.76715 + 1.92944(\log D_*) - 0.09815(\log D_*)^{2.0} - 0.00575(\log D_*)^{3.0} \\ &+ 0.00056(\log D_*)^{4.0}\end{aligned} \tag{S4}$$

where $W_{*0} = w_{*0}^3$ and $D_* = d_*^3$. Equation S4 is valid within the range of $0.05 \le D_* \le 5 \times 10^9$.

Figure S1

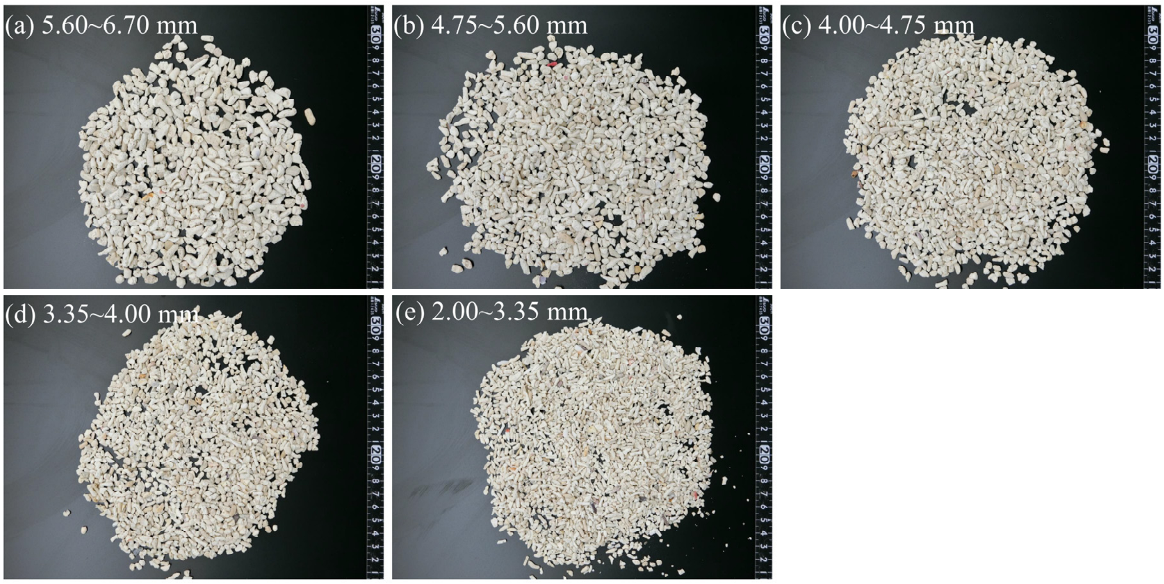

Figure S1. Photographs of the five coral debris fractions sorted through sieving.

Figure S2

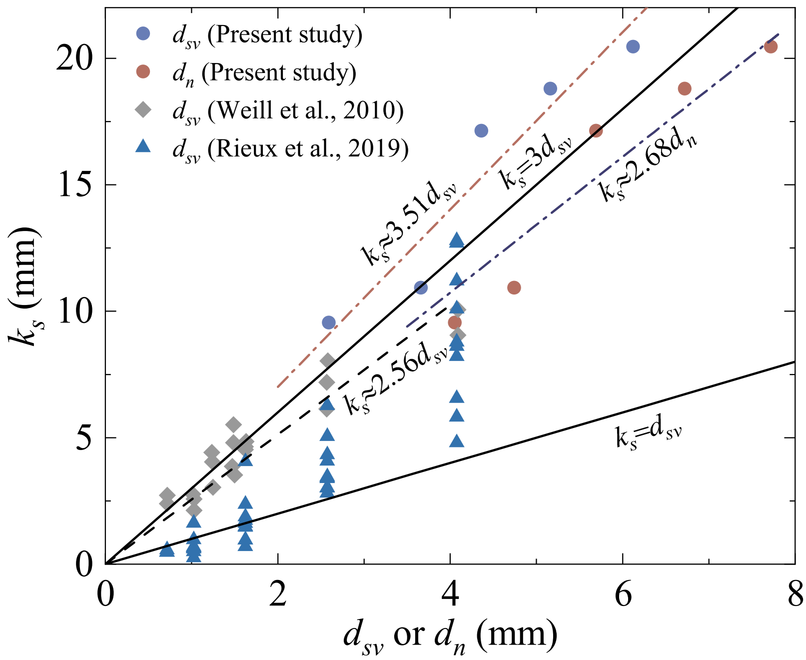

Figure S2. The Nikuradse roughness length k_s as a function of sieve diameter d_{sv} or nominal diameter d_n for the five coral debris beds. In this graph, the correlations between k_s and d_{sv} reported by Weill et al. (2010) and Rieux et al. (2019) are also plotted.

Figure S3

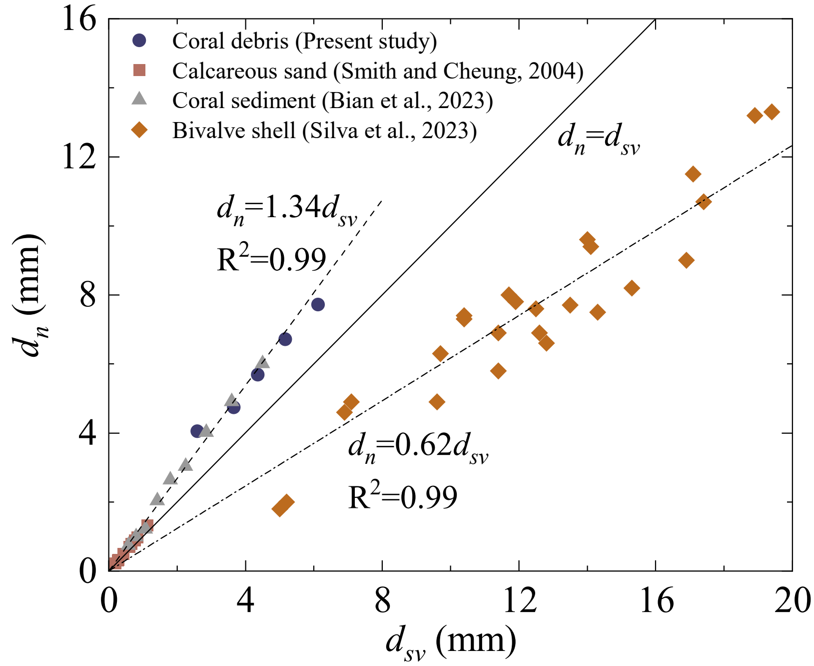

Figure S3. Correlation between the nominal diameter d_n and the sieve dimeter d_{sv} of investigated coral particles, calcareous sand (Smith and Cheung, 2004), coral sediment (Bian et al., 2023), and bivalve shells (Silva et al., 2023).

Figure S4

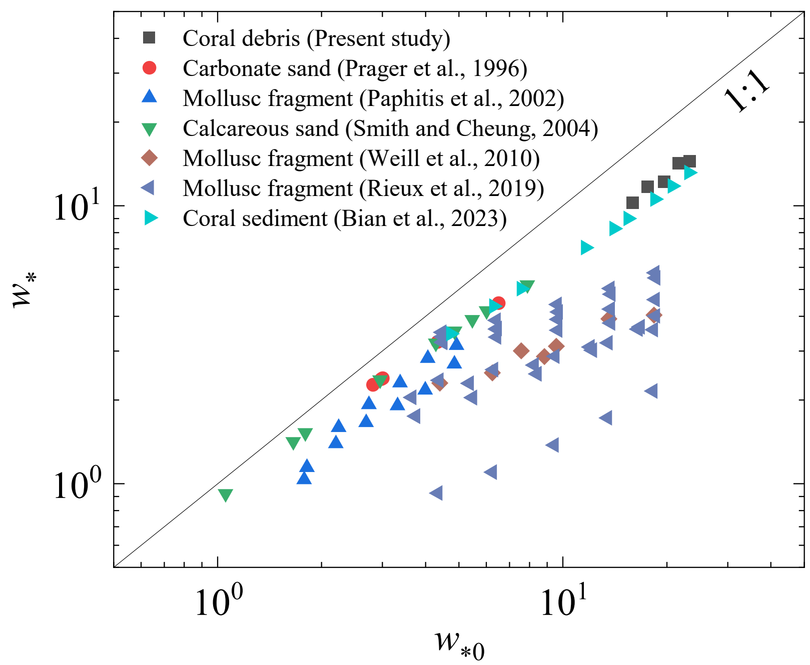

Figure S4. Correlation between w_* and the dimensionless settling velocity of a volume-equivalent sphere w_{*0} for considered bioclastic grains in this study.

Table S1. Experimental parameters at the entrainment threshold.

Sample	d_{sv} (mm)	d_n (mm)	A_{mp} (mm^2)	d_s/d_i	d_i/d_l	S_f	w_s (m/s)	$u_{*\mathrm{cr}}$ (×10^{-2} m/s)	Re_*	R_*	k_s (mm)	θ_{cr} (×10^{-2})	Λ_{c}
PS1	6.12	7.72	79.04	0.73	0.43	0.47	0.296	6.65	513.41	1360.8	20.46	6.67	0.22
PS2	5.16	6.72	58.11	0.76	0.43	0.49	0.291	5.67	380.83	1065.4	18.80	5.56	0.19
PS3	4.36	5.69	42.35	0.69	0.52	0.48	0.250	5.20	295.99	891.7	17.14	5.54	0.21
PS4	3.66	4.74	29.45	0.67	0.55	0.48	0.240	4.86	230.33	531.4	10.94	5.80	0.20
PS5	2.59	4.05	21.27	0.68	0.53	0.49	0.210	4.48	181.45	427.9	9.56	5.76	0.21

Table S2. Data compilation of threshold of motion of bioclastic sediments under steady current obtained from preceding studies.

Data source	Abbreviation	Number of data	Materials	Solid density (g/cm^3)	Used grain diameter	Shape factor	Settling velocity
Prager et al. (1996)	PR	5	Carbonate sand	2.50~2.73	d_{sv}	Not given	Not given
Paphitis et al. (2002)	PA	12	Mollusc fragment	2.72~2.80	d_{sv} and d_q	Not given	Given
Smith & Cheung (2004)	SC	9	Calcareous sand	2.60	d_{sv} and d_n	Not given	Not given
Weill et al. (2010)	WE	8	Mollusc fragment	2.60~2.71	d_{sv} and d_q	Not given	Given
Rieux et al. (2019)	RI	50	Mollusc fragment	2.01~2.80	d_{sv}	Not given	Given
Bian et al. (2023)	BI	45	Coral sediment	2.82	d_{sv} and d_n	S_f	Not given

*d_q is the equivalent settling diameter.

Table S3. Regression statistics and parameters for different scenarios. where $\boldsymbol{N}$ denotes the number of data used for regression, ARE is the absolute relative error, and $\boldsymbol{k}$ is the angular coefficient indicating the slope of the fitted line, with $\boldsymbol{k=1}$ denoting perfect agreement.

Data source	N	Scenarios			a	R^2	k	ARE (%)
		φ	d for calculating Λ_{c0}	F				
PS	5	0.42	d_n	1	—	0.997	0.778	22.11
PS	5	0.42	d_n	S_f	-0.344	0.997	1.002	3.67
PS	5	0.42	d_n	w_*/w_{*0}	-0.568	0.998	1.003	3.39
PS, SC	14	0.42 (PS), 0 (SC)	d_{sv}	1	—	0.995	0.778	18.21
PS, SC	14	0.42 (PS), 0 (SC)	d_n	1	—	0.993	0.799	14.46

PS, SC	14	0.42 (PS), 0 (SC)	d_n	w_*/w_{*0}	-0.560	0.995	1.012	9.37
PS, PR, PA, SC, WE, RI	89	0.42 (PS), 0 (others)	d_{sv}	1	—	0.862	0.554	35.64
PS, PR, PA, SC, WE, RI	89	0.42 (PS), 0 (others)	d_{sv}	w_*/w_{*0}	-0.589	0.972	0.935	14.81